FINAL REPORT FOR PERIOD: 8/15/95 to 8/15/96

1. Introduction

MAXIMUM is short for **M**ultiple **A**pplication **X**-ray **IM**aging **U**ndulator **M**icroscope, a project started in 1988 by our group at the Synchrotron Radiation Center of the University of Wisconsin-Madison. It is a scanning x-ray photoemission microscope that uses a multilayer-coated Schwarzschild objective as the focusing element. It was designed primarily for materials science studies of lateral variations in surface chemistry. Suitable problems include: lateral inhomogeneities in Schottky barrier formation, heterojunction formation, patterned samples and devices, insulating samples. Any system which has interesting properties that are not uniform as a function of spatial dimension can potentially be studied with MAXIMUM.

2. Microscope in Berkeley: 1995-present

Waiman Ng, then a postdoctoral fellow at the ALS, coordinated the move from LBNL's side and Sangeet Singh organized it from Madison. It was decided that, in continuation with our collaboration with the Center for X-ray Optics (CXrO), we would first install and test MAXIMUM on the CXrO bending magnet beamline BL6.3.2 at the Advanced Light Source and then move the microscope permanently to the CXrO undulator beamline BL12 upon its completion. An interim period at the ALS beamline BL7 was also foreseen.

2.1. Expected Improvement in Flux

We calculated the brightness of our old undulator at SRC and the undulators (5 cm gap at BL7, 8 cm gap at BL12) available at the ALS using the undulator simulation code !Urgent! written by J.P. Walker of the Sincrotrone Trieste. For three energies of interest, 80 eV, 130eV, and 180eV (reachable with Mo/Si, RuB_4C, and W/C multilayers, respectively) the brightness (units photons/s/mrad^2/mm^2/.1 % B.W.) was calculated for standard parameters. The 8 cm gap calculation was repeated for smaller values for the ALS emittances achieved in July 1995. Only the highest brightness results for each set of parameters is reported here. The parameters are summarized in Table 1. The brightnesses and factors of improvement over the SRC undulator are given in Table 2.

Parameters	*SRC I*	*SRC II*	*ALS I*	*ALS II*	*ALS III*
Period (cm)	6.1	6.1	5	8	8
Number of Periods	30	30	89	55	55
Electron Energy (GeV)	0.8	1	1.5	1.5	1.5
Current (Amps)	0.2	0.1	0.4	0.4	0.4
σ_x(mm)	0.85	1	0.21	0.21	0.0955
σ_y(mm)	0.063	0.135	0.04	0.04	0.0209
$\sigma_{x'}$(mrad)	0.19	0.24	0.019	0.019	0.0684
$\sigma_{y'}$(mrad)	0.015	0.02	0.01	0.01	0.0144

Table 1. Parameters for SRC and ALS undulators.

DISCLAIMER

hv	*SRC*	*ALS I*	*ALS II*	*ALS III*
80eV	$2.41x10^{15}$	$2.98x10^{17}$	$1.66x10^{17}$	$2.37x10^{18}$
	Improvement	123.47	68.83	981.56
130 eV	$2.45x10^{15}$	$1.05x10^{18}$	$5.29x10^{17}$	$2.95x10^{18}$
	Improvement	428.4	215.95	1205.27
180eV	$1.40x10^{15}$	$1.89x10^{18}$	$7.59x10^{17}$	$2.70x10^{18}$
	Improvement	1347.82	540.41	1919.91

Table 2. Maximal undulator brightness calculations for SRC and ALS undulators. The units of brightness are photons/s/mrad^2/mm^2/.1\%bw. The factors of improvement of ALS values over the highest SRC value are shown below the brightness values, with the largest factors in bold.

For 80eV, 130eV, and 180eV, the SRC I parameter set yielded the highest brightness values, at the first, second, and second undulator harmonics, respectively. The better designed ALS undulators achieved maximal brightness for the first harmonic for all three photon energies. As can be seen from Table 2, an increase in brightness of almost 2000 times can be expected for 180eV. For our current energy of 130eV, we expect to have an improvement of more than a factor of 1200 at BL12. This would translate into much faster data acquisition time and a higher accessible spatial resolution.

2.2. Move

We arranged for the move to be carried out by the Reynolds Transfer Company of Madison, Wisconsin, using an Air-Ride™ truck with an electronically controlled suspension system designed to minimize vibration.

The last date of MAXIMUM's operation at SRC was April 7, 1995 and moving day was 10 days away. The next day, a Saturday, Harun Solak and Sangeet Singh started disassembling the microscope piece by piece. In the following week, we drafted everyone we could find for help. We removed all optics, viewports, feedthroughs, and other delicate items. We disassembled and removed all items from the optics table. We then closed up all ports on all chambers with blanks and backfilled with dry nitrogen. Large items were fastened to pallets directly and small parts were packed with bubble wrap and put in boxes with more bubble wrap and foam peanuts. Everything was shipped out on Monday, April 17, 1995. Sangeet Singh left one day earlier to prepare to receive the microscope at LBNL. Once the shipment arrived, we put it in storage and unpacked, using this opportunity to take an inventory.

2.3. New Mounts

The ALS, a Department of Energy facility, has very stringent safety requirements. Because of the proximity of the Hayward Fault and other faults, one of these requirements concerns earthquake safety. To satisfy it, all experimental chambers must have massive mounts and that can survive shaking without causing harm. The chambers must be securely mounted on the mounts and the mounts must be secured to the laboratory floor. The ALS Experimental Systems Group generously agreed to finance the new stands for MAXIMUM. Engineer Pat McKean worked with us to come up with a design for the mounts. The design included a six strut alignment system consisting of three vertical struts for adjusting tilt and three horizontal struts for adjustments in the horizontal plane. A typical range of motion is 1-2 cm. Clearly an accurate initial positioning of the mounts is necessary in order to complete the alignment within this range. This is accomplished at the ALS using a fiducial system. In this system, a global coordinate system is used for measuring positions on the floor. Large fiducial marks in capped holes are put in the floor at regular intervals and small conical fiducial marks are welded in threesomes on all chambers positioned at beamlines. The survey team can take readings using these marks to determine the absolute position of the chambers. New endstations are designed according to this coordinate system so that they will be positioned in the right place with respect to the coordinates of the beamline. The final adjustment is often done together with the survey team. A positioning accuracy on the order of tens of microns is possible. After final positioning, holes are drilled in the floor and kinematic mounts are fixed in the holes with epoxy. Typically, pierced and threaded metal balls are positioned and fixed in the holes. The mating parts of the kinematic mounts on the stand rest on these balls and are screwed on, thus resulting in a rigid mounting.

Because the initial testing of MAXIMUM was to be carried out on BL6.3.2 on a periodic basis, it was important for the microscope to be portable. We decided to have the optical table equipped with jacks and wheels so that it could be

wheeled away after our beamtime. We also decided not to use vibration isolation any longer, but rather to mount everything rigidly and massively to minimize vibrations while ensuring that all components vibrate together, thus preventing relative motion that would adversely affect microscope performance. This approach had already been %%[Page: 1]%%~shown to be successf spectromicroscopes at the ALS. Portability for the prep-loadlock mount was accomplished by welding on slots for a forklift. The mount for the optics table holding the microscope is shown in Figure 1. The short spools under the vertical struts were put in to raise the microscope to the right position for the 66.5 in beam height at BL6.3.2 These will be removed when MAXIMUM is transferred to BL12.

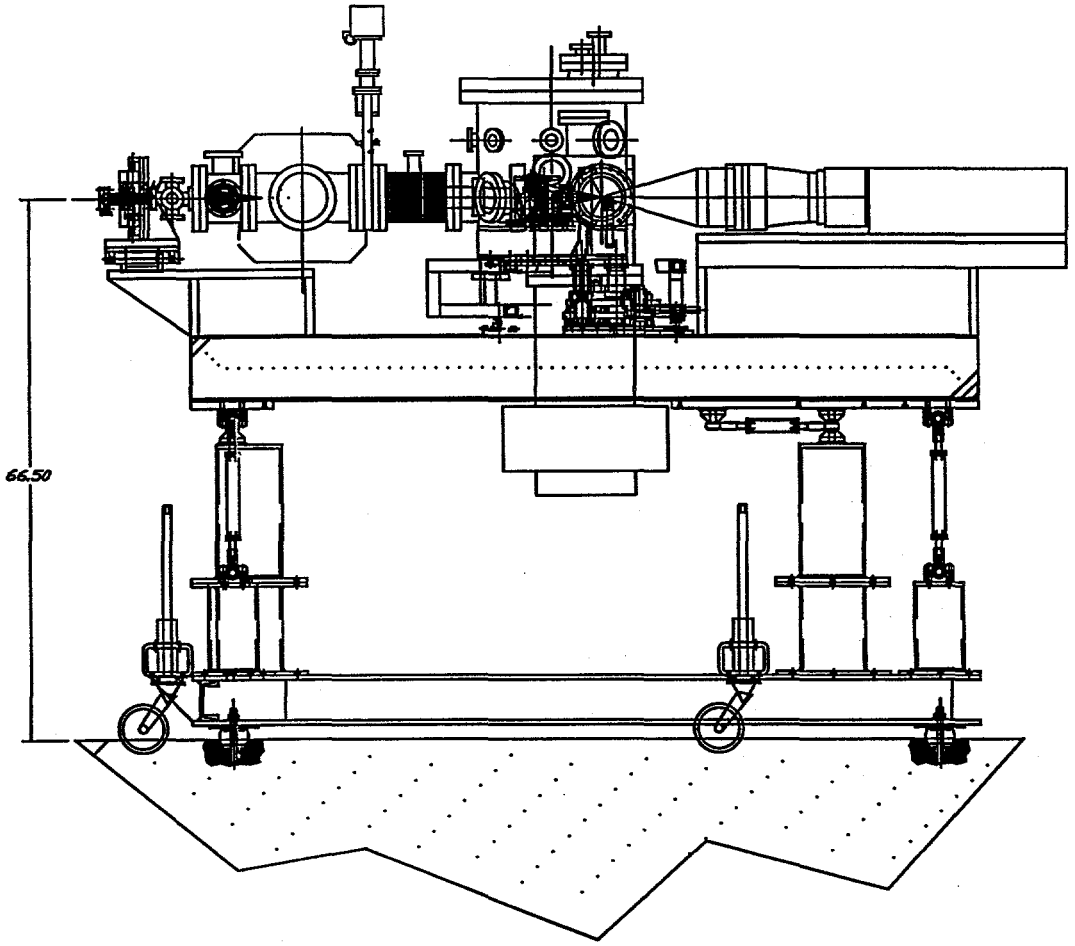

Figure 1. New six strut mounting system for the MAXIMUM microscope and its optical table.

2.4. ALS Beamline 6.3.2

In May 1995, we began to prepare for our first run at the ALS on BL6.3.2. This is a calibration and standards bending magnet beamline that uses a unique entrance slitless varied line spacing grating monochromator which corrects for aberrations in the preceding mirrors. It has a resolving power $\Delta\lambda/\lambda$ of about 7000. Three gratings (300, 600, and 1200 lines/mm) are available to access the photon energy range from 50 to 1000 eV. For our experiments we used the 300 lines/mm grating. The focus of the beamline is at the center of the reflectometer chamber endstation, at the location marked 'sample'. There is a sample stage on a goniometric mount that can be translated in three directions as well as rotated about an axis perpendicular to the beam. The reflectometer also has GaAsP and Si photodiodes that can be used to measure x-ray intensity. A LabView™ program is used to control the monochromator, read photocurrent off the refocusing mirror, and to move the reflectometer stage.

A holder was designed for mounting a pinhole on the reflectometer stage. This pinhole defined the source for MAXIMUM and would be demagnified by a factor of 20 onto the sample. To do this, the distance d_o between the pinhole and the primary mirror had to remain constant, beamline changes were necessary because the pinhole was in a separate chamber. The position of the microscope chamber with respect to the reflectometer is shown in Figure 3. The beamline had to be shortened by the radius of the reflectometer chamber, a distance of about 16 inches. We did this by removing several 2.75 inch tees and crosses previously used at SRC for feedthroughs for Au photodiodes, mirrors, and beam splitters. This meant also not having an optical microscope. Because the reflectometer's lowest pressure is $2x10^{-8}$ Torr and a pressure two orders lower is required in the MAXIMUM microscope chamber, differential pumping was needed. Unfortunately, there was no space in the beamline to install a tee with small apertures and a small ion pump. We compromised by getting a special short 2.75 inch bellows made into the end of which we lodged a short cylindrical plug with a through hole 1 cm in diameter to limit the conductance between the two chambers. We also constructed new supports for the ion pumps. Because our stay at BL6.3.2 was to be a temporary one, the balls for the kinematic mount holes drilled into the floor were not epoxied in place. Instead, the microscope stand's kinematic mounts simply rested on the balls, and the entire stand was tied down to the floor using thick metal bars and threaded rods fed into holes tapped into the floor. The final configuration of the microscope on this beamline was captured on film and is shown in Figure 2.

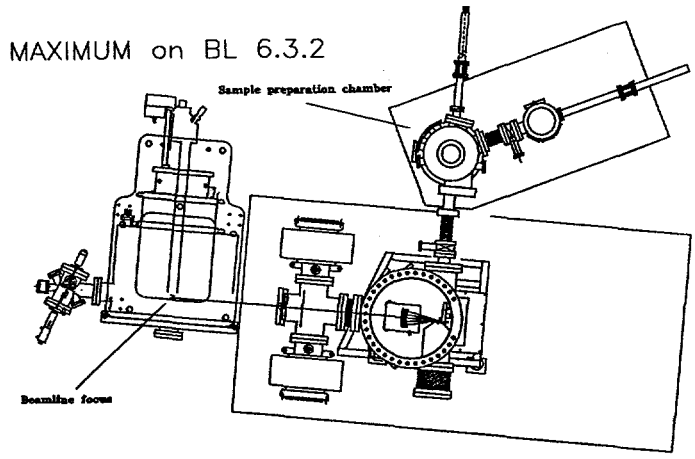

Figure 2. MAXIMUM microscope chamber positioned at ALS Beamline BL6.3.2 to obtain the proper distance d_o between the pinhole and the Schwarzschild objective's primary mirror. The pinhole is positioned at the reflectometer focus.

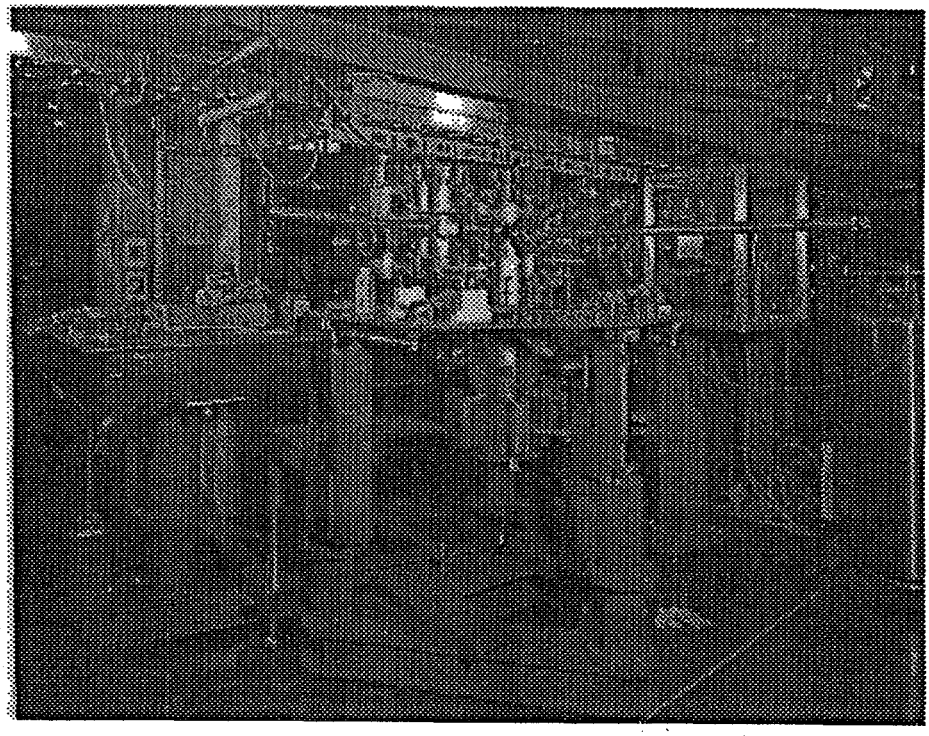

Figure 3. The MAXIMUM microscope chamber as assembled on ALS Beamline BL6.3.2. Both the optics table and prep-loadlock mounts are in place.

2.4.1. Qualification Run

In August 1995, we carried out some preliminary experiments to test and characterize the performance of MAXIMUM at ALS Beamline 6.3.2. For aligning the Schwarzschild objective for this first run we performed an *in situ* star test using the 0th order visible light from the bending magnet. A spot size of 0.5μm was to be attained at the focus with the 10μm pinhole. Unfortunately, the inchworm controlling the gap between the two mirrors became stuck in one position before alignment was complete, and had to push it manually in order to get the focus spot downstream enough to hit the sample. We did not have enough beamtime to spare to open up the 22 inch top flange and attempt repairs, and thus decided to proceed with an imperfect alignment. In this incarnation of MAXIMUM we did not install the preparation and loadlock chambers and did not bake out the microscope. Despite these limitations, we were able to obtain a resolution of 1.25μm in photoemission mode on a patterned wafer using a 100 μm pinhole. Interestingly the bending magnet flux here at a third generation synchrotron was comparable to the flux obtained on an undulator at the second generation ring Aladdin at SRC. A photon energy of '129.3' eV was used because the x-ray flux to the sample was highest at this energy.[1]

[1] The change from the '132.5 eV' used at SRC may result from the way the monochromator is calibrated and the energy calculated. It may also arise from a difference in illumination of the Schwarzschild objective. Different wavelengths have a maximal reflectivity on different annular regions of the (spherical) Schwarzschild objective mirrors. '129.3 eV' did so on ALS BL6.3.2.

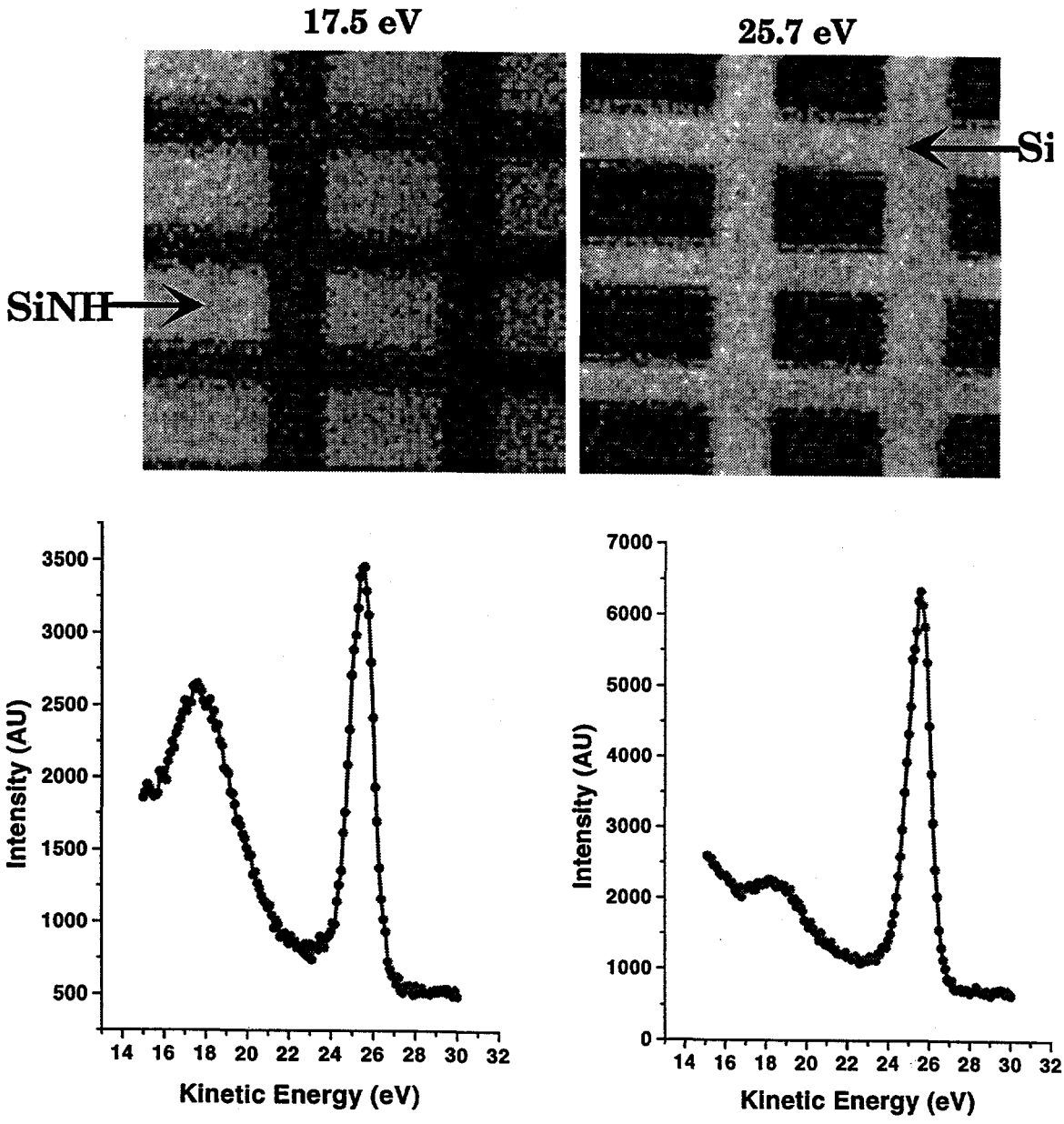

Figure 4. 80 μm x 80 μm x 1μm step images of SiNH pads on Si. The left image was acquired at the shifted Si 2p peak. Charging leads to the magnitude of the shitf. In this image the nitride pads appear bright. The right image was acquired on the clean Si 2p peak. In this image the Si areas between the SiNH pads appear bright.

Sangeet Singh carried out an experiment on a SiNH/Si patterned sample similar to the one depicted in Figure 4 this time using MAXIMUM's ability to image local differences in the surface chemistry of a chemically etched Si wafer patterned with 922 Å thick silicon nitride features. Such a sample is stable even at non-UHV pressures.[2] Figure 5 shows a partial yield image of the sample. Energy distribution curves (EDCs) taken on Si and SiNH regions of the sample show a dramatic chemical difference. These are shown in Figure 6a and Figure 6b, respectively. The sample was subjected to a light chemical cleaning by immersion in 1 % HF for ~ 4 minutes followed by a ~ 2 minute rinse with deionized H_2O. It was then put into the experimental chamber and pumped down within 15 minutes. When a pressure of $1x10^{-7}$ Torr was reached (after ~ 1 hour), the focused x-ray spot was positioned at the corner of a SiNH feature on the Si substrate. Figure 5 shows an

[2] Stoichiometrically, silicon nitride can be represented by the formula Si_3N_4. However, the silicon nitride formed in practice does not conform to this formulation. The nitride is often also in a hydrogenated state, regardless of the method of formation. In this paper the expression SiNH will be used to refer to silicon nitride.

80 μm x 80 μm image of that region acquired with a step size of 1μm at a photoelectron energy of 0 eV. The bright raised square corresponds to the nitride feature and the surrounding area corresponds to the silicon substrate. An EDC acquired on the Si region is shown in Figure 6a after background removal and curve fitting with Gaussian functions. Figure 6b shows the EDC taken on the SiN region. The fitting parameters are summarized in Table 3.

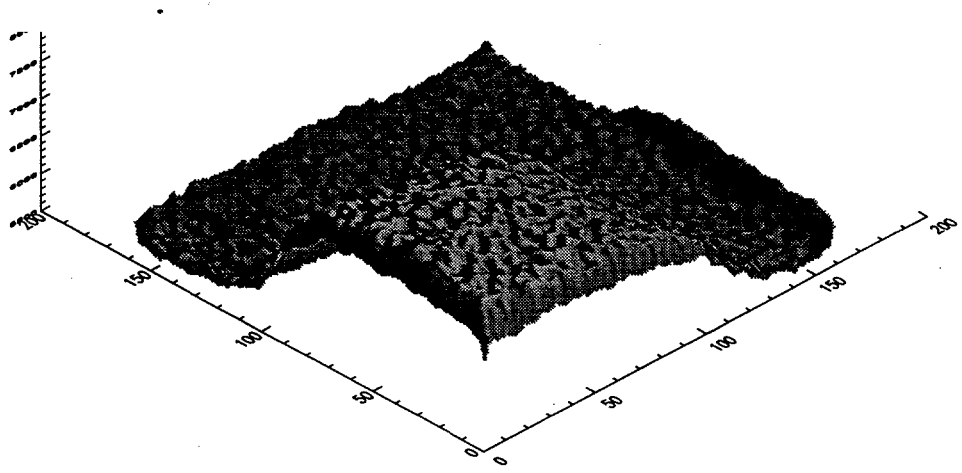

Figure 5. Secondary electron 80 μm x 80 μm image of a pad of SiNH on Si. The raised square is a SiNH feature and the surrounding area is the Si substrate.

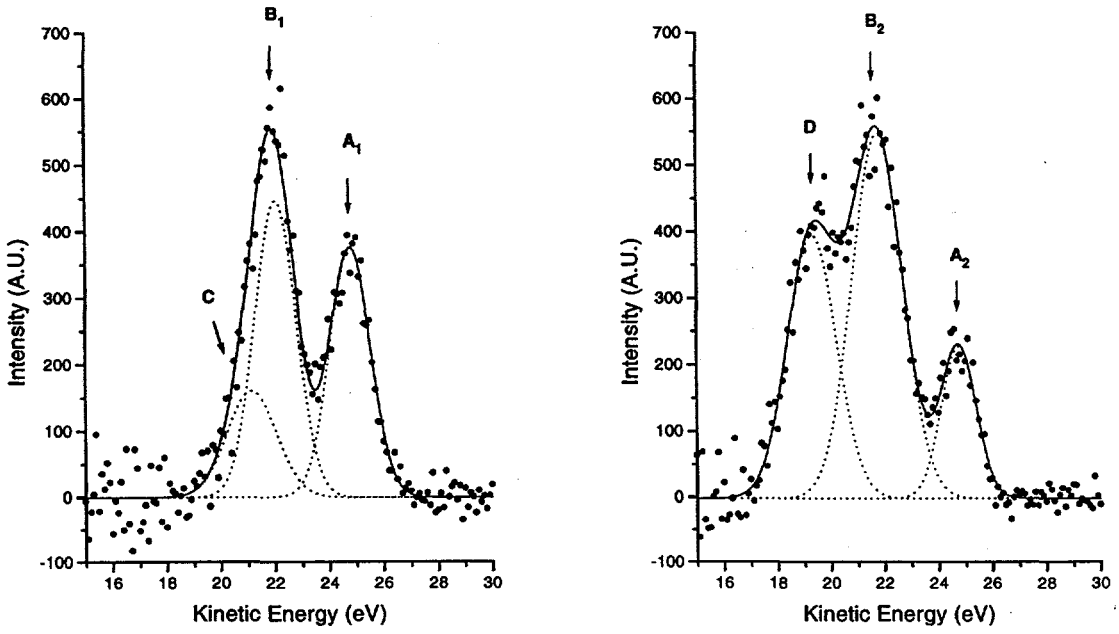

Figure 6. Si 2p EDC acquired on the Si area of Figure 5 is shown in (a). The peaks A_1, B_1, and C correspond, respectively, to clean Si, Si_2O_3, and SiO_2. (b) shows the corresponding spectrum acquired on the SiNH feature Peaks A_2, B_2, and D are assigned to clean Si, Si_2O_3 (tentatively), and SiNH, respectively.}

Parameters	*Silicon*	*Silicon Nitride*
Energy of Peak 1 (eV)	24.8	24.8
Shift of Peak 2 (eV)	-2.8	-3.0
Shift of Peak 3 (eV)	-3.7	-5.5
FWHM of Peak 1 (eV)	1.5	1.3
FWHM of Peak 2 (eV)	1.5	1.9
FWHM of Peak 3(eV)	1.8	1.8
Intensity of Peak 1 (A.U.)	376	228
Intensity of Peak 2 (A.U.)	446	547
Intensity of Peak 3 (A.U.)	161	395

Table 3. Gaussian fitting parameters for EDCs acquired on the silicon and silicon nitride areas of the image.

In both EDCs Peak 1 corresponds to the 2p core level of Si. The energy resolution of the system is not sufficient to allow the$2p_{3/2}$ and $2p_{1/2}$ components to be distinguished. The main peak is found to be at a kinetic energy of 24.8eV. Figure 5a shows that two other peaks, B_1 at 22.0 eV and C at 21.1eV, are found in addition to A_1 on the chemically cleaned Si. Notwithstanding the noise in the data and the difficulty in obtaining a perfect fit, these peaks can be assigned, tentatively, to the Si^{+3} and Si^{+4} oxidation states of Si since 0.8eV - 0.9eV of chemical shift can be attributed to each bond a Si atom has with an oxygen atom, with the shift for SiO_2 ranging from 3.6eV to 4.4eV. The SiO_2 peak is also broadened as expected. The intensity of the clean Si is lower than that of the oxide peaks since the chemical clean was not sufficiently thorough. It is well known that the oxidation of HF etched Si not only proceeds more slowly than that of annealed Si but also results in the preferential formation of the lower oxidation state oxides Si_2O, SiO, and Si_2O_3 over SiO_2.The lower oxidation state oxides form first also on annealed Si. This is consistent with the lowered rate of oxidation of HF cleaned Si. The presence of SiO_2 on our sample can partially be explained by the incomplete removal of the native oxide present on the Si wafer by the light HF etch carried out. A stronger HF etch for 20 - 30 minutes would have been more effective. Cleaner equipment and purer solutions are also essential in avoiding contamination of the wafer during cleaning. However, the fact that the silicon dioxide chemical shift is at the lower end of the range at -3.6eV rather than the -4.0eV typical of the native oxide may indicate that strain at the Si/SiO_2 interface may be lowering Si-O bonding energies. In this case, incomplete removal of the native oxide is not implicated.

Figure 6b shows the two shifted peaks B_2 and D in addition to the clean Si peak A_2 on the EDC taken on the SiNH feature. Peak D at 19.3eV is not present in the EDC acquired on the Si substrate and has been observed on SiNH in past experiments on SiNH as well. It can be assigned to SiNH although the nominal chemical shift for stoichiometric SiNH is only 2.7 eV because of local charging of the almost 0.1 μm thick nitride layer and the fact that the exact chemical composition of the SiNH in this sample is not known. Peak B_2 at 21.7 eV may arise from Si_2O_3 although its chemical shift of -3.0eV is 0.2eV off from the expected shift of Si_2O_3 on Si. This oxide of silicon may have resulted from a contamination layer formed on the surface of the SiNH during ion implantation of the sample after nitride patterning and that was not completely removed during the chemical cleaning, which, after all, is designed for Si, not HF.

That this is indeed the case is evidenced by the fact that Peak B_2 was not present on SiNH in an experiment on an identical sample cleaned by flash heating to ~1100 °C in UHV, which results in the removal of material from the entire surface of the sample. Data from that sample were shown in Figure 4 above. The unshifted Si 2p peak in that experiment is different because of differences in termination of the dangling bonds on the Si surface. In the flash-cleaned sample, the surface is very sensitive and easily pinned. In the HF-cleaned sample, the Si surface is supposedly H-terminated and stable, even at room pressure. In UHV, it is stable indeed, as evidenced by the fact that the spectra don't change even when the sample is left in UHV for 2-3 days! In the current experiment, both peaks are widened as expected for chemically shifted components. The fraction of signal from clean Si is expectedly lower for a SiNH sample, but the fraction of SiNH signal is lower than that of the silicon oxide because of the incomplete chemical clean. Clearly, more detailed studies need to be done to better understand the chemical etching of the Si/SiNH system and resolve some of the issues discussed above. These results were presented at the 1995 Synchrotron Radiation Instrumentation conference.